PAPER

Mechanistic insights into rare-earth-catalysed C–H alkylation of sulfides: sulfide facilitating alkene insertion and beyond†

Yu Zhou, Ping Wu, Fanshu Cao, Lei Shi, Ni Zhang, Zuqian Xue and Gen Luo [ID] *

The catalytic C–H alkylation with alkenes is of much interest and importance, as it offers a 100% atom efficient route for C–C bond construction. In the past decade, great progress in rare-earth catalysed C–H alkylation of various heteroatom-containing substrates with alkenes has been made. However, whether or how a heteroatom-containing substrate would influence the coordination or insertion of an alkene at the catalyst metal center remained elusive. In this work, the mechanism of Sc-catalysed C–H alkylation of sulfides with alkenes and dienes has been carefully examined by DFT calculations, which revealed that the alkene insertion could proceed *via* a sulfide-facilitated mechanism. It has been found that a similar mechanism may also work for the C–H alkylation of other heteroatom-containing substrates such as pyridine and anisole. Moreover, the substrate-facilitated alkene insertion mechanism and a substrate-free one could be switched by fine-tuning the sterics of catalysts and substrates. This work provides new insights into the role of heteroatom-containing substrates in alkene-insertion-involved reactions, and may help guide designing new catalysis systems.

Introduction

Developing efficient methodologies for synthesis and functionalization of sulfides is of great interest and importance, as sulfide motifs exist widely and play important roles in bioactive molecules, natural products, functional materials, and organocatalysts.[1] The most straightforward and atom-economical route for the synthesis of alkylated sulfide derivatives is the catalytic C–H alkylation of sulfides with alkenes. However, such C–H alkylation approaches met with limited success,[2] and in most cases only alkenes with an electron-withdrawing group showed reactivity. Recently, Hou and coworkers reported that half-sandwich scandium catalysts such as $(C_5Me_5)Sc(CH_2C_6H_4NMe_2\text{-}o)_2$ could serve as a unique platform for the C–H alkylation of a wide range of methyl sulfides with various alkenes and dienes, which represents the first example of regioselective catalytic α-C(sp^3)–H addition of sulfides to unactivated alkenes (Scheme 1a).[3] Based on experimental observations, a possible reaction mechanism was proposed as shown in Scheme 1b. The C–H activation of the methyl group of sulfide **1** by the cationic scandium monoalkyl species **A**, which was generated by the reaction of the scandium dialkyl complex with $[Ph_3C][B(C_6F_5)_4]$,[4] could give an intermediate **I** as the

catalytically active species. In the reaction with α-alkenes (Scheme 1b, left), the insertion of an alkene **2** into the Sc–C bond in **I** would give **II**, which after the protonation (C–H activation) of another sulfide **1** would release the hydrothiomethylation product **3** and regenerate the active species **I**. In the case of 1,5-dienes (Scheme 1b, right), starting from **I**, the reaction would proceed through sequential insertion of the two C=C bonds and the subsequent protonation, giving the corresponding thiomethyl-functionalized cyclopentane derivative **3′**. It is also worth noting that a significant kinetic isotope effect (KIE ≈ 5) was observed experimentally, which suggests that C–H activation of the methyl group in the sulfides should be involved in the rate-determining step.[3]

Although the above proposed mechanism could schematically explain the products obtained experimentally, many details remained unclear, such as structural information on the active catalyst species, key intermediates and transition states, the energy profiles of the reaction processes, and rationale for the observation that C–H activation is the rate-determining step. Moreover, although the C–H functionalization of various heteroatom-containing substrates with alkenes catalysed by rare-earth complexes have been widely reported,[5–11] whether or how a heteroatom-containing substrate would influence the coordination or insertion of an alkene at the catalyst metal center remained elusive. In order to clarify these important issues, we performed density functional theory (DFT) studies on the Sc-catalysed C–H alkylation of sulfides with alkenes and dienes. We found that alkene insertion took place through a sulfide-facilitated mechanism, preferably

Institutes of Physical Science and Information Technology, Anhui University, Hefei 230601, China. E-mail: luogen@ahu.edu.cn
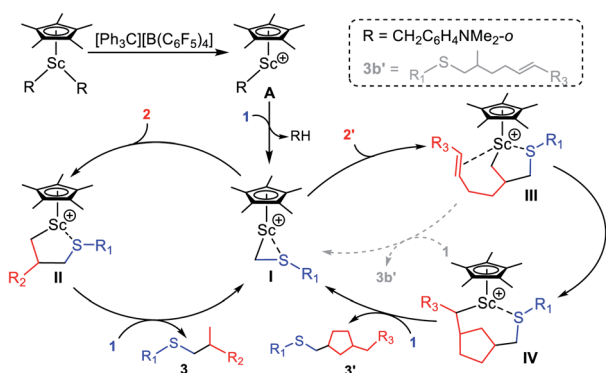
† Electronic supplementary information (ESI) available: Distortion–interaction analysis, other energy profiles, coordinates of all optimized structures. See https://doi.org/10.1039/d2ra02180c
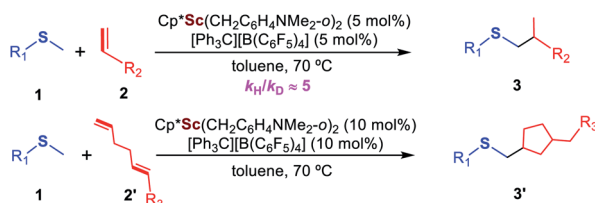
Scheme 1 (a) Sc-catalysed α-C–H functionalization of sulfides with alkenes and dienes and (b) proposed mechanism.

proceeding at a catalyst species bearing a sulfide ligand. Moreover, the C–H alkylation of other heteroatom-containing substrates such as anisoles and pyridines with alkenes may also take place through the similar mechanism. In addition, it is also noting that the substrate-facilitated alkene insertion mechanism and the substrate-free one could be switched by combining different factors, such as substrate, catalyst ligand, metal center and so on. These new findings reported here clearly revealed the role of the heteroatom-containing substrate

and effectively enrich the mechanism of rare-earth catalyzed C–H functionalization.

Computational details

Geometry optimizations and frequency calculations of all structures were performed with Gaussian 16 software package[12] at the B3PW91 (ref. 13)/BSI level. In BSI, the 6-31G(d) basis set was considered for C, H, O, N, and S atoms, and SDD[14] basis sets were used for Sc, Y, and Lu (MWB60) atoms. The frequency calculations confirmed a stationary point as a minimum (no imaginary frequency) or a transition state (one imaginary frequency) and obtained the thermodynamic corrections to Gibbs free energy (298.15 K, 1 atm). Intrinsic reaction coordinate (IRC) calculations were performed to verify a direct connection between two minima for a transition state. All structures were optimized without any symmetry restrictions. To obtain more reliable relative energies, single-point energy calculations were performed at the level of M06 (ref. 15)/BSII with SMD implicit solvent model[16] for considering solvation effect of toluene. In BSII, the 6-311+G(d,p) basis set was used for all nonmetal atoms, and SDD basis sets were used for Sc, Y, and Lu (MWB60) atoms. The theoretical strategy adopted here has been successfully applied in similar systems.[10] In addition, several other widely used functional/basis set/solvation model combinations have also been tested for key processes and no significant effect on the obtained results was observed (see Fig. S6†), suggesting the reliability of the current calculation strategy. In this work, relative Gibbs free energies in toluene solution (including gas-phase corrections) were used to discuss reaction pathways. Distortion–interaction analysis[17] of transition states and natural bond orbital (NBO) calculations were performed at the M06/BSII level. Three-dimensional molecular graphics were visualized with CYLview software.[18]
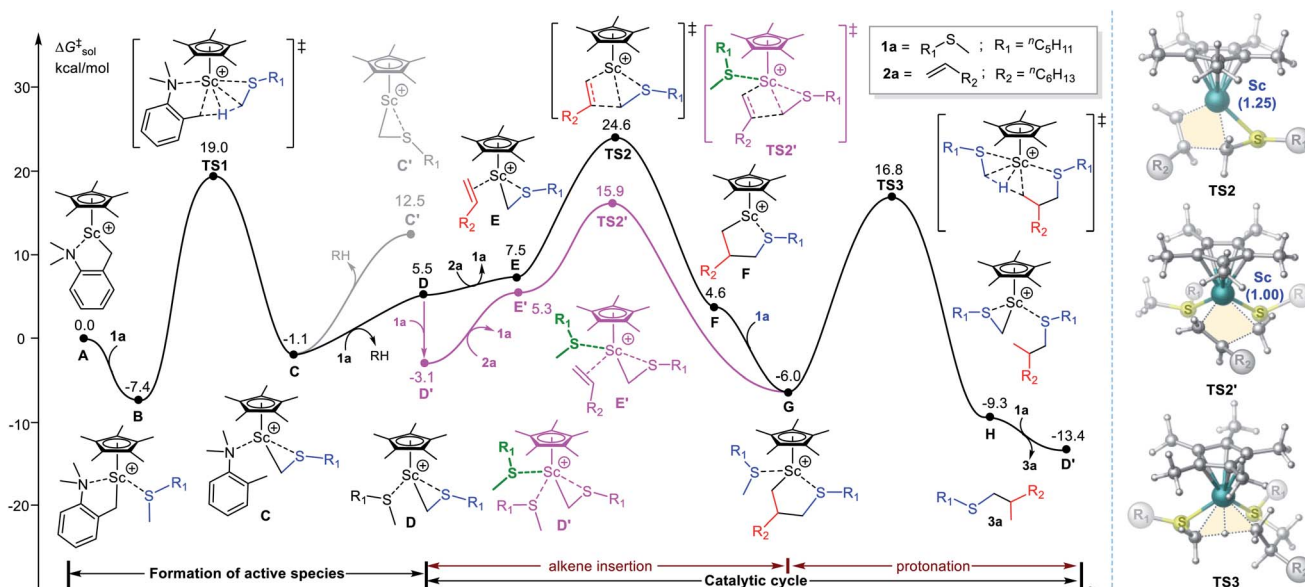

Fig. 1 Energy profile for Sc-catalysed C–H alkylation of $^nC_5H_{11}SMe$ (**1a**) with 1-octene (**2a**) calculated at the level of M06/6-311+G(d,p)/SDD (toluene, SMD)//B3PW91/6-31G(d)/SDD. The natural charge of the metal center (Q_{Sc}) is given in blue with parentheses.

Paper

Results and discussion

Some possible reaction processes and energy profile of the Sc-catalysed α-C–H alkylation of $^nC_5H_{11}SMe$ (**1a**) with 1-octene (**2a**)[3] are shown in Fig. 1. The reaction proceeds through the coordination of the sulfur atom of **1a** to the Sc atom in the cationic scandium species **A**, giving an adduct **B**. The following C–H activation of the α-methyl group in the coordinated **1a** via the transition state **TS1** ($\Delta G^{\ddagger} = 26.4$ kcal mol^{-1}) could form a three-membered metallacycle intermediate **C** with an *N,N*-dimethyl-*o*-toluidine (RH) moiety. In addition, the N-dissociated pathway of the C–H activation by coordinating another **1a** was calculated to overcome a high energy barrier (via **TS1′**, Fig. S1†). This is mainly due to the stronger Sc···N interaction than Sc···S one based on HSAB theory, which makes the

N-ligated pathway more favourable (via **TS1**, Fig. 1). For comparison, the C–H activation of the α-methylene group in **1a** is also considered and calculated to be unfavourable due to steric hindrance (Fig. S2†). The release RH from **C** generates the proposed naked cationic scandium species **C′** with a high relative free energy ($\Delta G = 12.5$ kcal mol^{-1}), so it should be excluded. Alternatively, the ligand exchange between **1a** and RH in **C** could easily occur to form the species **D** with a coordinated **1a**.[11c–e] Starting from **D**, the ligand exchange between **2a** and **1a** could take place to form a π-complex **E**. Subsequently, the alkene ligand in **E** may insert into the Sc–C bond via **TS2** ($\Delta G = 24.6$ kcal mol^{-1}) to give the five-membered ring intermediate **F**, as proposed in literature.[3] The re-coordination of a sulfide **1a** to the Sc atom easily takes place to give the more stable species **G**. The protonation of the Sc–alkyl bond via C–H activation of the coordinated-**1a** in **G** would finally release the alkylation product **3a**.

It is noted that alkene insertion transition state **TS2** has the highest free energy in potential energy surface. In addition, we noted that the coordination of one more molecule of **1a** to **D** could give a more stable species **D′** ($\Delta G = -3.1$ kcal mol^{-1}). Further coordinated sulfides will lead to an increase in energy because of steric factors (see Fig. S3† for more details). According to the energetic span model,[19] therefore, the species **D′** with two coordinated sulfides should be regarded as the catalytically active species and the energy barrier of the alkene insertion via **TS2** should be 27.7 kcal mol^{-1} (**D′** → **TS2**). However, the energy barrier is significantly higher than that of the subsequent C–H activation process in **G** (via **TS3**, $\Delta G^{\ddagger} = 22.8$ kcal mol^{-1}). This is not in agreement with the experimental observation of a significant kinetic isotope effect (KIE ≈ 5),
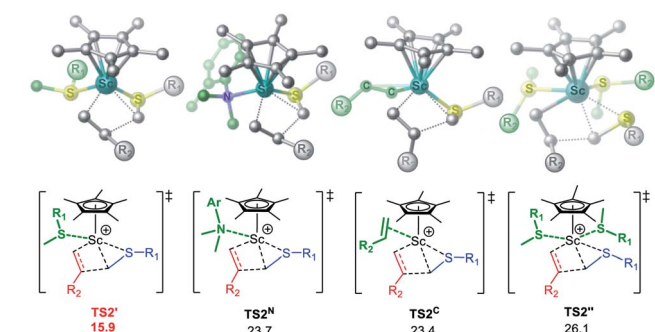

Fig. 2 Calculated transition states of alkene insertion assisted by different coordination molecules ($R_1 = {}^nC_5H_{11}$; $R_2 = {}^nC_6H_{13}$; Ar = *o*-Me-phenyl). Relative free energies are given in kcal mol^{-1}. All H atoms in 3D structures are omitted for clarity.
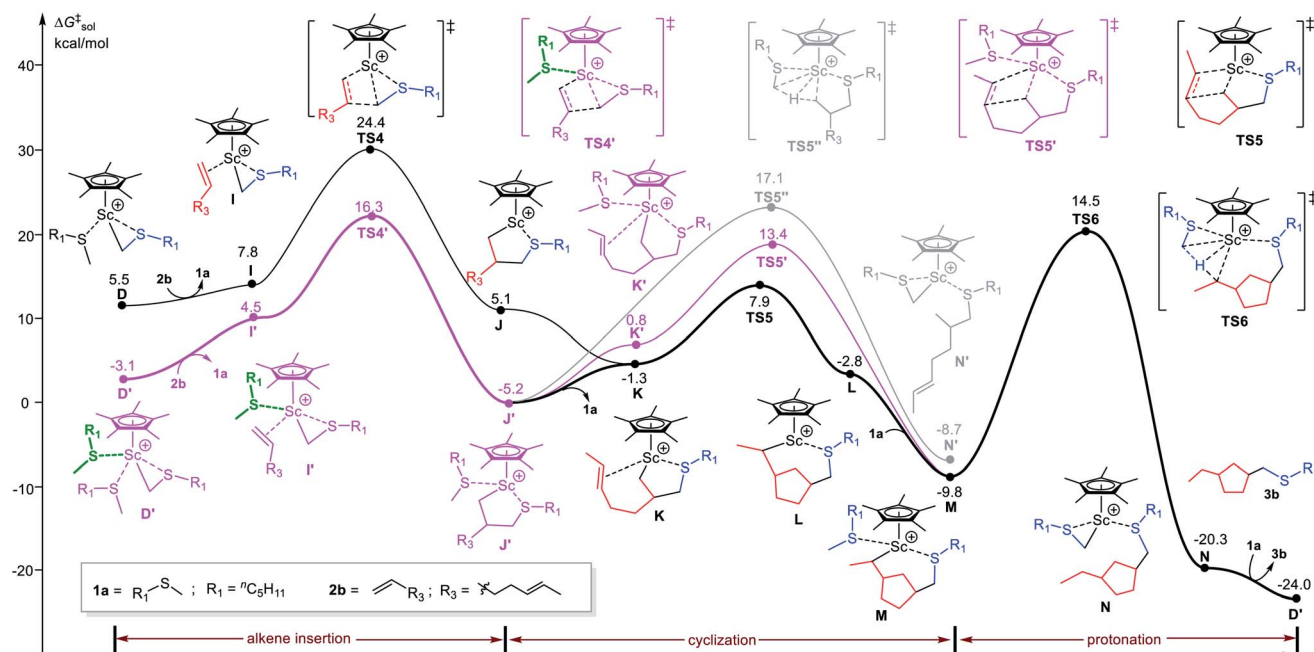

Fig. 3 Energy profile for Sc-catalyzed C–H alkylation of $^nC_5H_{11}SMe$ (**1a**) with 1,5-heptadiene (**2b**). The free energies (kcal mol^{-1}) are relative to the species **A** as shown in Fig. 1.

which suggested that the C–H activation of the methyl group in the sulfide should be involved in the rate-determining step.[3]

We then try to explore other potential routes for alkene insertion. Notably, considering that the unique heteroatom affinity of rare-earth metal center and the opening coordination space in the structure of **TS2**, it encourages us to examine whether the alkene insertion can be accomplished with the aid of a molecule of sulfide. To our delight, the alkene insertion significantly reduces in energy by the assistance of a sulfide *via* 1,2-insertion transition state **TS2′**,[20] because the coordination of a sulfide ligand would lower the positive charge of the Sc center ($Q_{Sc} = 1.25$ in **TS2** *vs.* $Q_{Sc} = 1.00$ in **TS2′**) and thereby stabilize the transition state. Consequently, the energy barrier of alkene insertion can be reduced from 27.7 to 19.0 kcal mol^{-1} (**D′** → **TS2′**, Fig. 1, pink line) instead of being a rate-determining step. In addition, the alkene insertion assisted by other potential

coordinating molecules in current system (*i.e.*, *N*,*N*-dimethyl-*o*-toluidine and 1-octene) as well as assisted by two sulfides were also considered and were ruled out due to higher relative energies (Fig. 2). Therefore, the newly established sulfide-facilitated mechanism seems more reasonable and could well explain the experimental result of KIE. We also calculated the KIE for C–H activation,[21] in which the CH$_3$ group to be activated in C–H activation was replaced by CD$_3$. The computed KIE of 4.57 *via* **TS3** matches the experimental datum (KIE ≈ 5),[3] which provides further support for the mechanism scenario here. The computational results suggest that the reaction mainly involve the formation of catalytically active species, alkene insertion, and protonation steps. To be noted, the active species should be a cationic scandium species with two coordinated sulfide molecules (**D′**) rather than the proposed cationic species without sulfide (**C′**)[3,11a,b] or with one coordinated sulfide

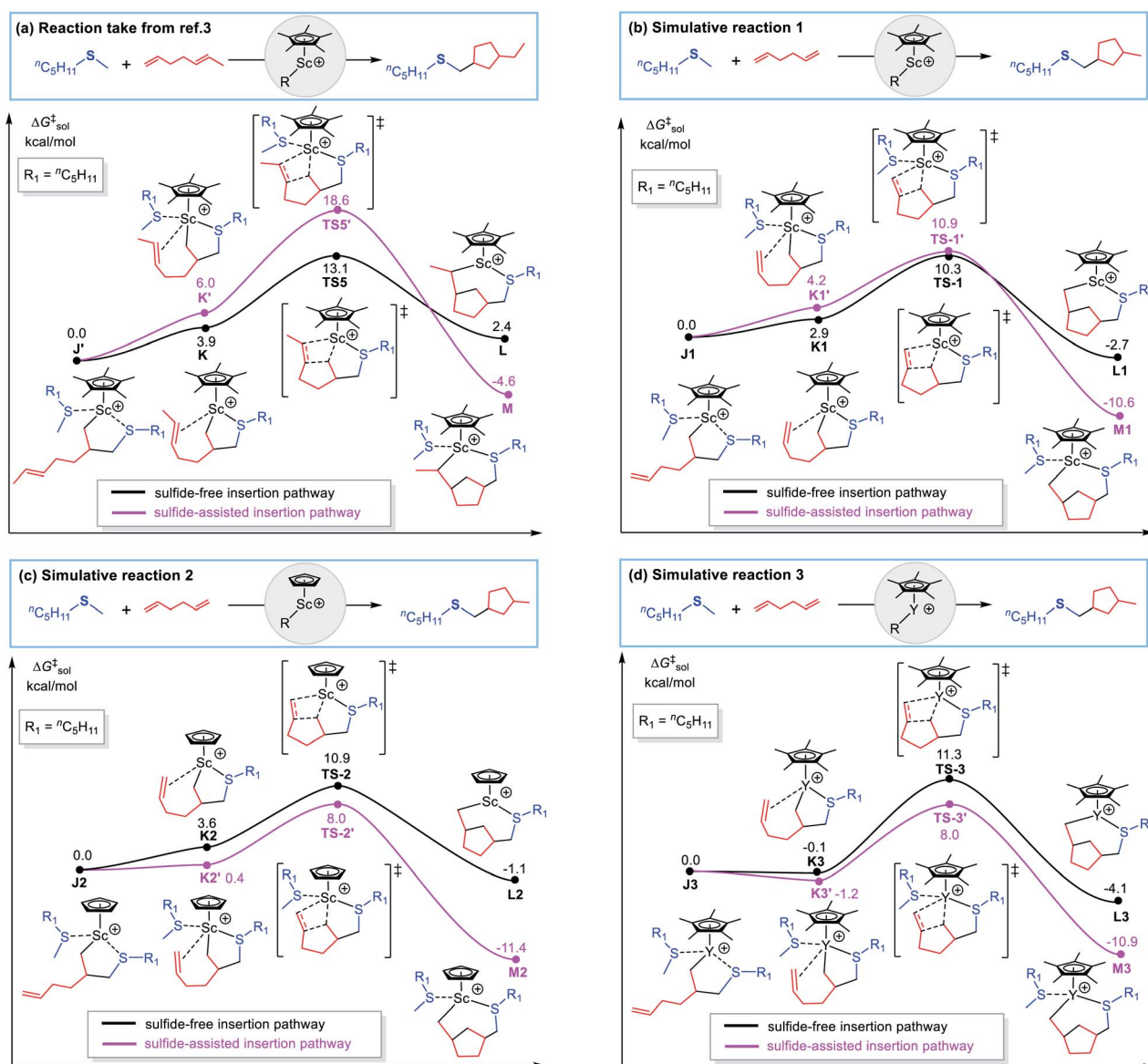**Fig. 4** Energy profiles for cyclization processes for the case of 1,5-heptadiene catalyzed by (C$_5$Me$_5$)ScR$_2$ (a) and the case of 1,5-heptadiene catalysed by (C$_5$Me$_5$)ScR$_2$ (b), (C$_5$H$_5$)ScR$_2$ (c), and (C$_5$Me$_5$)YR$_2$ (d), respectively.

reported previously (**D**).[11c–e] The sulfide substrate not only involves in C–H activation processes (the formation of active species and the final protonation) but also serves as a Lewis acidic ligand to stabilize related intermediates and transition states in alkene insertion process.

With such a sulfide-facilitated mechanism in hand, we turn to the mechanism of C–H alkylation of sulfides with unconjugated dienes. The reaction of 1,5-heptadiene (**2b**) with $^nC_5H_{11}$-SMe (**1a**) giving thiomethyl-functionalized cyclopentane product **3b** was computationally investigated (Fig. 3). Similar in the case of 1-octene, the terminal C=C double bond insertion occurs through the sulfide-facilitated mechanism (*via* **TS4′**) is significantly favourable than the sulfide-free pathway (*via* **TS4**) by 8.1 kcal mol^{-1}. By contrast, the following C=C insertion (cyclization) in **J′** takes place through a sulfide-free pathway (**TS5**) instead of the sulfide-facilitated mechanism (**TS5′**) due to steric effects (*vide infra*). It is worth noting that the direct protonation of Sc–alkyl bond in **J′** by hydrogen abstraction of the coordinated **1a** *via* **TS5″** needs to overcome an energy barrier of 22.3 kcal mol^{-1} (Fig. 2, gray line), which is much higher than that of the cyclization process (*via* **TS5**, $\Delta G^{\ddagger} = 13.1$ kcal mol^{-1}). This is well in line with the experimental observation of the exclusive formation of the thiomethylated cyclopentane product rather than a simple alkylation product with a free olefinic bond. The results clearly show that, in the case of diene, the reaction operates through the sulfide-facilitated alkene insertion, followed by the sulfide-free alkene insertion (cyclization) and protonation steps to complete catalytic cycle. The C–H activation is the rate-determining step, as in the case of 1-octene.

To have a better understand of the discrepancy of mechanism for the two sequential alkene insertion processes mentioned above, we performed more calculations on alkene insertion (cyclization) processes by modifying diene or catalyst

(ligand and metal center). The results are shown in Fig. 4b–d, and the case of 1,5-heptadiene catalysed by $(C_5Me_5)ScR_2$ is illustrated again in Fig. 4a for comparison. As shown in Fig. 4b, by reducing steric hindrance of diene, the sulfide-facilitated alkene insertion mechanism and the sulfide-free one become competitive with each other when 1,5-hexadiene is used instead of 1,5-heptadiene in the $(C_5Me_5)Sc$-catalysed cyclization process. When the steric hindrance is further reduced by using the scandium catalyst with smaller ligand C_5H_5 (Fig. 4c) or the C_5Me_5-ligated catalyst with the larger yttrium or lutetium center (than scandium) (Fig. 4d and S5†), it obviously shows that the sulfide-facilitated mechanism becomes more favourable than the sulfide-free pathway. Therefore, these results clearly indicate that the mechanisms of alkene insertion could be switched by tuning the sterics, including substrate, catalyst ligand, metal center and so on. There is a subtle balance between steric and electronic factors, leading to different mechanisms. When the catalyst–substrate combined structure has less steric hindrance, it prefers to undergo heteroatom-containing substrate facilitated alkene insertion mechanism due to the heteroatom affinity of rare-earth metal center. On the contrary, the heteroatom-containing substrate-free mechanism is more likely to occur. These findings are helpful for us to better understand how the heteroatom-containing substrate influence the coordination and insertion of an alkene at the catalyst center and are also expected to guide the design of new rare-earth catalysis reactions.

To examine the potential applicability of the heteroatom-containing substrate facilitated alkene insertion mechanism, we extended the investigation to C–H alkylation of *O*-(anisole)[8a] and *N*-containing (pyridine)[6a] substrates with alkenes catalysed by the same scandium catalyst $(C_5Me_5)Sc(CH_2C_6H_4NMe_2\text{-}o)_2$ (Fig. 5) as used in the sulfide system.[3] It is found that, in the case of anisole (Fig. 5, left), the alkene insertion *via* the anisole-free
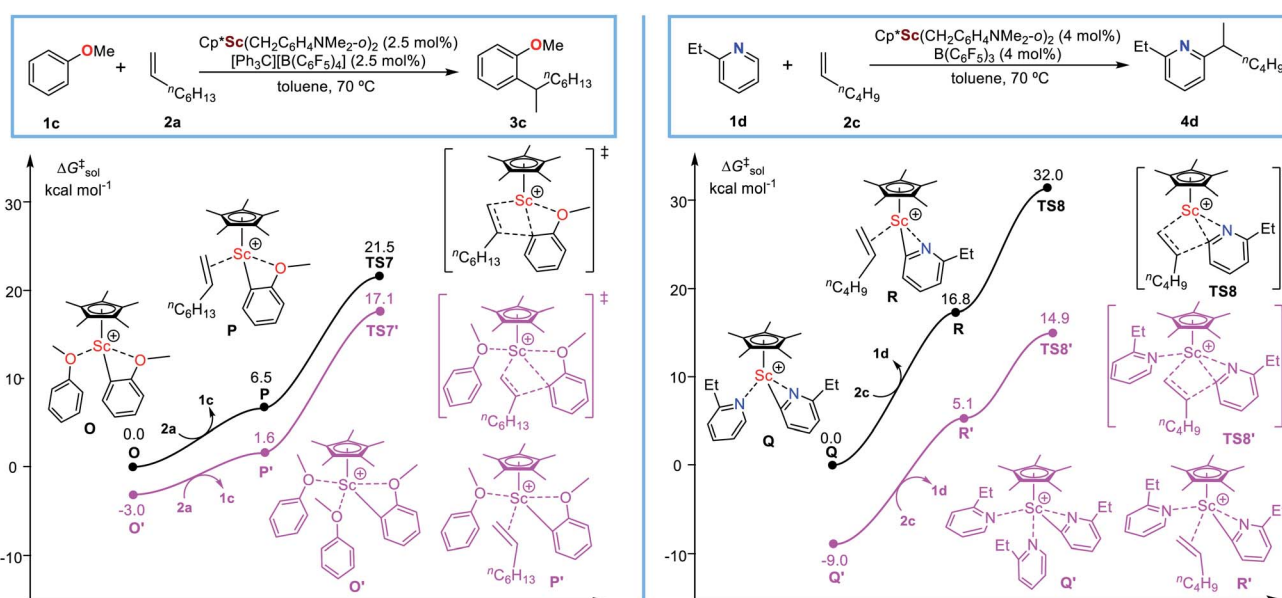

Fig. 5 Energy profile for alkene insertion processes involved in Sc-catalysed C–H alkylation of other heteroatom (N and O)-containing substrates with alkenes.

pathway (**TS7**) has a relative free energy of 21.5 kcal mol^{-1}, while the anisole-facilitated pathway *via* **TS7$'$** has a relative free energy of 17.1 kcal mol^{-1}. Therefore, similar to the sulfide system, the anisole-facilitated alkene insertion mechanism is much more favourable than the anisole-free mechanism in the Sc-catalysed C–H alkylation of anisole system. As expected, in the case of pyridine, similar results are obtained that alkene insertion undergoes the pyridine-facilitated mechanism (Fig. 5, right), which remind us to modify the previously proposed mechanism of C–H alkylation of pyridines with alkenes.[11a,b]

The result suggests that the heteroatom-containing substrate facilitated alkene insertion mechanism potentially has wide applicability in the field of rare-earth catalysed C–H alkylation, which is complementary or modified to those mechanisms proposed previously[5a,11] and thus effectively enrich the mechanism framework of rare-earth catalysed C–H functionalization chemistry. In addition, it is worth mentioning that Cui, Hou, and Marks groups reported the interaction between the heteroatom (*e.g.*, N, O, P, S, Se) in functionalized olefin monomer and the rare-earth catalyst could significantly improve the polymerization activity.[22] The promotion effect of the heteroatom in olefin polymerization (continuous alkene-insertion-involved reactions) is similar to that in the C–H alkylation systems discussed here. Therefore, the heteroatom-containing substrate facilitated alkene insertion mechanism is also expected to apply in polymerization of heteroatom-functionalized olefins.

Conclusions

In summary, the mechanism of Sc-catalysed C–H alkylation of sulfides with alkenes and dienes has been carefully examined by DFT calculations. The results suggest that the reaction mainly involves several steps: the formation of catalytically active species, alkene insertion (sequential insertion for diene), and protonation. The catalytically active species is the cationic species with two coordinated sulfide molecules rather than the sulfide-free or one sulfide coordinated cationic species proposed previously. Interestingly, it is found that the alkene insertion takes place through a sulfide-facilitated mechanism, during which the sulfide substrate serves as a ligand to stabilize key intermediates and transition states in alkene insertion process. More importantly, such a substrate-facilitated alkene insertion mechanism also works for Sc-catalysed C–H alkylation of other heteroatom (O and N)-containing substrates. The promotion effect of the heteroatom-containing substrate on alkene insertion is obviously complementary or modified to those mechanisms proposed previously. In addition, the results also show that the substrate-facilitated alkene insertion mechanism and the substrate-free one could be switched by fine-tuning the sterics of catalysts and substrates. The new insights into the role of heteroatom-containing substrate on alkene insertion and the adjustable mechanisms not only greatly enrich the mechanism framework of rare-earth catalysed C–H functionalization chemistry but also may help guide designing new catalysis systems.

Conflicts of interest

There are no conflicts to declare.

Acknowledgements

Notes and references

1 (*a*) D. Poirier, S. Auger, Y. Mérand, J. Simard and F. Labrie, *J. Med. Chem.*, 1994, **37**, 1115–1125; (*b*) D. Meng, W. Chen and W. Zhao, *J. Nat. Prod.*, 2007, **70**, 824–829; (*c*) Z. Ke, C. K. Tan, F. Chen and Y.-Y. Yeung, *J. Am. Chem. Soc.*, 2014, **136**, 5627–5630; (*d*) M. Nakano and K. Takimiya, *Chem. Mater.*, 2017, **29**, 256–264.

2 (*a*) J. Chen, R. L. Kirchmeier and J. M. Shreeve, *Inorg. Chem.*, 1996, **35**, 6676–6681; (*b*) W.-T. Wei, M.-B. Zhou, J.-H. Fan, W. Liu, R.-J. Song, Y. Liu, M. Hu, P. Xie and J.-H. Li, *Angew. Chem., Int. Ed.*, 2013, **52**, 3638–3641; (*c*) H. Yang, H. Yan, P. Sun, Y. Zhu, L. Lu, D. Liu, G. Rong and J. Mao, *Green Chem.*, 2013, **15**, 976–981; (*d*) H. Cao, D. Liu, C. Liu, X. Hu and A. Lei, *Org. Biomol. Chem.*, 2015, **13**, 2264–2266; (*e*) S. Kamijo, G. Takao, K. Kamijo, T. Tsuno, K. Ishiguro and T. Murafuji, *Org. Lett.*, 2016, **18**, 4912–4915; (*f*) D. Xia, Y. Li, T. Miao, P. Li and L. Wang, *Green Chem.*, 2017, **19**, 1732–1739; (*g*) Y.-F. Liu, L. Zheng, D.-D. Zhai, X.-Y. Zhang and B.-T. Guan, *Org. Lett.*, 2019, **21**, 5351–5356.

3 Y. Luo, Y. Ma and Z. Hou, *J. Am. Chem. Soc.*, 2018, **140**, 114–117.

4 X. Li, M. Nishiura, K. Mori, T. Mashiko and Z. Hou, *Chem. Commun.*, 2007, 4137–4139.

5 For reviews, see: (*a*) M. Nishiura, F. Guo and Z. Hou, *Acc. Chem. Res.*, 2015, **48**, 2209–2220; (*b*) R. D. Dicken, A. Motta and T. J. Marks, *ACS Catal.*, 2021, **11**, 2715–2734.

6 For examples of rare-earth catalysed C–H bond addition of pyridines to alkenes, see: (*a*) B.-T. Guan and Z. Hou, *J. Am. Chem. Soc.*, 2011, **133**, 18086–18089; (*b*) B.-T. Guan, B. Wang, M. Nishiura and Z. Hou, *Angew. Chem., Int. Ed.*, 2013, **52**, 4418–4421; (*c*) G. Song, W. W. N. O and Z. Hou, *J. Am. Chem. Soc.*, 2014, **136**, 12209–12212; (*d*) G. Song, B. Wang, M. Nishiura and Z. Hou, *Chem.–Eur. J.*, 2015, **21**, 8394–8398; (*e*) Y. Luo, H.-L. Teng, M. Nishiura and Z. Hou, *Angew. Chem., Int. Ed.*, 2017, **56**, 9207–9210; (*f*) Y. Chen, D. Song, J. Li, X. Hu, X. Bi, T. Jiang and Z. Hou, *ChemCatChem*, 2018, **10**, 159–164.

7 For examples of rare-earth catalysed C–H bond addition of anilines to alkenes, see: (*a*) X. Xu, X. Zheng and X. Xu, *ACS Catal.*, 2021, **11**, 14995–15003; (*b*) J. Su, Y. Luo and X. Xu,

Chem. Commun., 2021, **57**, 3688–3691; (*c*) J. Su, Y. Cai and X. Xu, *Org. Lett.*, 2019, **21**, 9055–9059; (*d*) H. Gao, J. Su, P. Xu and X. Xu, *Org. Chem. Front.*, 2018, **5**, 59–63; (*e*) G. Song, G. Luo, J. Oyamada, Y. Luo and Z. Hou, *Chem. Sci.*, 2016, **7**, 5265–5270.

8 For examples of rare-earth catalysed C–H bond addition of anisoles to alkenes, see: (*a*) J. Oyamada and Z. Hou, *Angew. Chem., Int. Ed.*, 2012, **51**, 12828–12832; (*b*) B. Tang, X. Hu, C. Liu, T. Jiang, F. Alam and Y. Chen, *ACS Catal.*, 2019, **9**, 599–604; (*c*) X. Shi, M. Nishiura and Z. Hou, *J. Am. Chem. Soc.*, 2016, **138**, 6147–6150.

9 For examples of rare-earth catalysed C–H bond addition of aldimines/amines to alkenes, see: (*a*) X. Cong, G. Zhan, Z. Mo, M. Nishiura and Z. Hou, *J. Am. Chem. Soc.*, 2020, **140**, 5531–5537; (*b*) X. Cong, Q. Zhuo, N. Hao, Z. Mo, G. Zhan, M. Nishiura and Z. Hou, *Angew. Chem., Int. Ed.*, 2022, **61**, e202115996; (*c*) A. Nako, J. Oyamada, M. Nishiura and Z. Hou, *Chem. Sci.*, 2016, **7**, 6429–6434.

10 For examples of rare-earth catalysed C–H bond addition of quinolines to alkenes/alkynes, see: (*a*) S.-J. Lou, G. Luo, S. Yamaguchi, K. An, M. Nishiura and Z. Hou, *J. Am. Chem. Soc.*, 2021, **143**, 20462–20471; (*b*) S.-J. Lou, Q. Zhuo, M. Nishiura, G. Luo and Z. Hou, *J. Am. Chem. Soc.*, 2021, **143**, 2470–2476; (*c*) S.-J. Lou, L. Zhang, Y. Luo, M. Nishiura, G. Luo, Y. Luo and Z. Hou, *J. Am. Chem. Soc.*, 2020, **140**, 18128–18137.

11 Theoretical studies on rare-earth catalysed C–H alkylation with alkenes, see: (*a*) G. Luo, Y. Luo, J. Qu and Z. Hou, *Organometallics*, 2012, **31**, 3930–3937; (*b*) G. Zhou, G. Luo, X. Kang, Z. Hou and Y. Luo, *Organometallics*, 2018, **37**, 2741–2748; (*c*) F. Liu, G. Luo, Z. Hou and Y. Luo, *Organometallics*, 2017, **36**, 1557–1565; (*d*) G. Luo, F. Liu, Y. Luo, G. Zhou, X. Kang, Z. Hou and L. Luo, *Organometallics*, 2019, **38**, 1887–1896; (*e*) P. Wang, G. Luo, J. Yang, X. Cong, Z. Hou and Y. Luo, *J. Org. Chem.*, 2021, **86**, 4236–4244.

12 M. J. Frisch, G. W. Trucks, H. B. Schlegel, G. E. Scuseria, M. A. Robb, J. R. Cheeseman, G. Scalmani, V. Barone, G. A. Petersson, H. Nakatsuji, X. Li, M. Caricato, A. V. Marenich, J. Bloino, B. G. Janesko, R. Gomperts, B. Mennucci, H. P. Hratchian, J. V. Ortiz, A. F. Izmaylov, J. L. Sonnenberg, D. Williams-Young, F. Ding, F. Lipparini, F. Egidi, J. Goings, B. Peng, A. Petrone, T. Henderson, D. Ranasinghe, V. G. Zakrzewski, J. Gao, N. Rega, G. Zheng, W. Liang, M. Hada, M. Ehara, K. Toyota, R. Fukuda, J. Hasegawa, M. Ishida, T. Nakajima, Y. Honda, O. Kitao, H. Nakai, T. Vreven, K. Throssell, J. A. Montgomery Jr, J. E. Peralta, F. Ogliaro, M. J. Bearpark, J. J. Heyd, E. N. Brothers, K. N. Kudin, V. N. Staroverov, T. A. Keith, R. Kobayashi, J. Normand, K. Raghavachari, A. P. Rendell, J. C. Burant, S. S. Iyengar, J. Tomasi, M. Cossi, J. M. Millam, M. Klene, C. Adamo, R. Cammi, J. W. Ochterski, R. L. Martin, K. Morokuma, O. Farkas, J. B. Foresman and D. J. Fox, *Gaussian 16, Revision A.03*, Gaussian, Inc., Wallingford, CT, 2016.

13 (*a*) A. D. Beck, *J. Chem. Phys.*, 1993, **98**, 5648–5652; (*b*) J. P. Perdew and Y. Wang, *Phys. Rev. B: Condens. Matter Mater. Phys.*, 1992, **45**, 13244–13249.

14 M. Dolg, U. Wedig, H. Stoll and H. Preuss, *J. Chem. Phys.*, 1987, **86**, 866–872.

15 Y. Zhao and D. G. Truhlar, *Theor. Chem. Acc.*, 2008, **120**, 215–241.

16 A. V. Marenich, C. J. Cramer and D. G. Truhlar, *J. Phys. Chem. B*, 2009, **113**, 6378–6396.

17 For reviews, see: (*a*) I. Fernández and F. M. Bickelhaupt, *Chem. Soc. Rev.*, 2014, **43**, 4953–4967; (*b*) F. Liu, Y. Liang and K. N. Houk, *Acc. Chem. Res.*, 2017, **50**, 2297–2308; (*c*) F. M. Bickelhaupt and K. N. Houk, *Angew. Chem., Int. Ed.*, 2017, **56**, 10070–10086.

18 C. Y. Legault, *CYLview, 1.0b*, Université de Sherbrooke, 2009, https://www.cylview.org.

19 S. Kozuch and S. Shaik, *Acc. Chem. Res.*, 2011, **44**, 101–110.

20 The insertion of 1-octene into Sc-alkyl bond *via* 1,2-fashion is more favourable than 2,1-mode due to electronic factors (Fig. S4†), also see ref. 11*a* and *c*.

21 The semiclassical KIE was calculated using the Eyring model, $\text{KIE} = k_H/k_D = \exp[(\Delta G_D^{\ddagger} - \Delta G_H^{\ddagger})/RT]$, in which the free energy barriers ($\Delta G^{\ddagger}$) were calculated at the level of M06/6-311+G(d,p)/SDD (toluene, SMD)//B3PW91/6-31G(d)/SDD (298.15 K), see: Y. Sun, H. Tang, K. Chen, L. Hu, J. Yao, S. Shaik and H. Chen, *J. Am. Chem. Soc.*, 2016, **138**, 3715–3730.

22 (*a*) D. Liu, C. Yao, R. Wang, M. Wang, Z. Wang, C. Wu, F. Lin, S. Li, X. Wan and D. Cui, *Angew. Chem., Int. Ed.*, 2015, **54**, 5205–5209; (*b*) C. Wang, G. Luo, M. Nishiura, G. Song, A. Yamamoto, Y. Luo and Z. Hou, *Sci. Adv.*, 2017, **3**, e1701011; (*c*) J. Chen, Y. Gao, B. Wang, T. L. Lohr and T. J. Marks, *Angew. Chem., Int. Ed.*, 2017, **56**, 15964–15968.